Electronic Supporting Information

A fast and selective probe for detection of CN⁻ and F⁻ in water along with sequential molecular logic circuit *via* resettable optical readout

Alok Kumar Singh*

Department of Chemistry, University of Delhi, Delhi-110 007, India.

E-mail: aloksinghchemistry@gmail.com

Material and Methods: The majority of salts for sensing experiment were purchased from BDH chemicals Ltd, Sigma Adrich and used as received. 2-Acetyl pyridine, pyridine-4-carboxaldehyde, $FeCl_2$ and NH_4PF_6 were purchased from Sigma-Aldrich and used as received. Ethanol and acetonitrile (HPLC grade) were purchased from Merck and distilled using reported methods.[S1] Deuterated solvents were purchased from Sigma Aldrich and stored under freezer. Water used for the experiment was double distilled. UV-vis spectra were recorded using an analytikjena SPECORD 250 with a quartz cuvette (path length = 1 cm, volume = 3 ml). Fluorescence spectroscopy experiments were performed on Varian Cary eclipse fluorescence instrument (slit width, 5 nm) with a quartz cuvette (path length, 1 cm). IR spectra were recorded on Perkin-Elmer FT-IR spectrophotometer in range 400-4000 cm^{-1} using KBr as a medium. All ^1H-NMR spectra were recorded on Jeol JNMECX 400p spectrometer at room temperature using DMSO-d_6. All chemical shifts (δ) were recorded in ppm with reference to TMS and coupling constant (J) in Hz. The pH of the solution was fixed with EUTECH Instruments pH 510, calibrated with buffer solution of pH 4.00 and 9.00 before each measurement. The pH of test solution was adjusted with $\sim 10^{-3}$ M HCl and NaOH solution in H_2O. The optical probe **1** was synthesised following only some alteration in the reported synthetic method (Scheme 1).[S2] The ligand 4'-pyridyl-2,2':6',2''-terpyridine (pytpy) was prepared according to a reported procedure resulting in needle shaped white crystals.[S3]
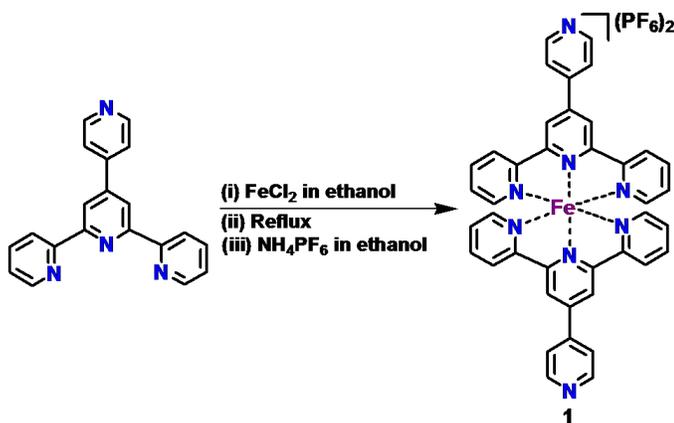
Scheme 1: Synthetic scheme for the preparation of probe **1**.

Synthesis of optical probe (1). The ligand 4'-pyridyl-2,2':6',2''-terpyridine (pytpy) (156.7 mg, 0.50 mmol) was dissolved in 25 mL of hot ethanol and then $FeCl_2$ (32.1 mg, 0.25 mmol) in 10 mL ethanol was added dropwise with constant stirring under a N_2 atmosphere. The reaction-mixture was refluxed with stirring for 4 h. After cooling to room temperature, the reaction-mixture was filtered, subsequently, **1** was precipitated out by the addition of saturated ethanolic solution of NH_4PF_6 and collected by vacuum filtration. The residue was washed with an ample amount of water followed by diethyl ether, dried under vacuum and recrystallized using a mixture of acetonitrile and water resulting in a purple colour microcrystalline solid. Yield: 148.7 mg (61%). ^{1}H-NMR (400 MHz, DMSO-d_6): δ (ppm) = 9.78 (s, 4H, H$_{3'}$), 9.05 (m, 8H, H$_{m+3}$), 8.53 (d, J = 6.3 Hz, 4H, H$_o$), 8.06 (t, J = 8.1 Hz, 4H, H$_4$), 7.28 (d, J = 5.9 Hz, 4H, H$_6$), 7.19 (t, J = 6.9 Hz, 4H, H$_5$); ^{13}C-NMR (400 MHz, DMSO-d_6, δ): 160.25, 157.64, 152.90, 151.05, 146.24, 143.16, 138.96 127.75, 124.30, 121.74, 121.30; IR (KBr): υ (cm^{-1}) = 558 (m), 836 (vs), 1408 (m), 1598 (m); TOF-MS (m/z, calculated for $C_{40}H_{28}F_{12}N_8P_2Fe$): 821 [M-PF$_6$]$^+$, 338 [M-2PF$_6$]$^{2+}$; UV-vis (10^{-5} M, CH$_3$CN): λ = 569 nm (ε = 22,931 M^{-1} cm^{-1}); CV (vs. Ag/AgCl): E$_{1/2}$ = 1.24 V (Fe$^{2+/3+}$), ΔE = 70 mV at 300 mVs^{-1}.
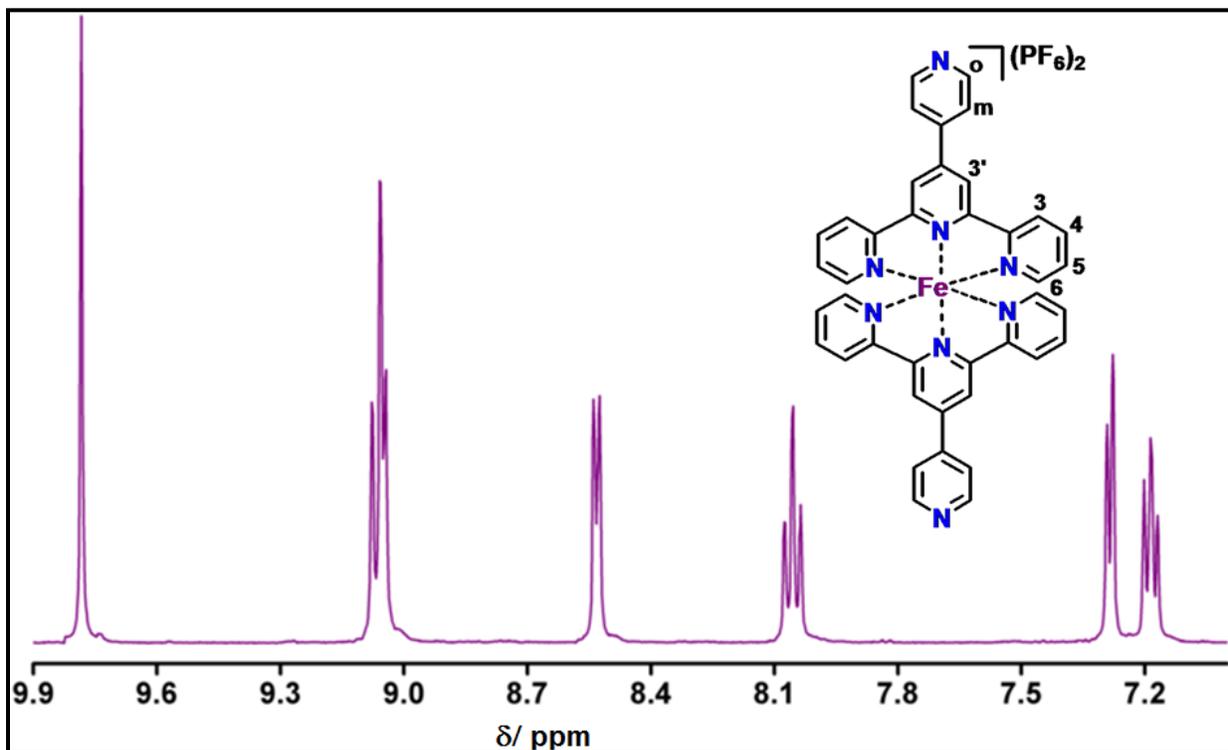
Figure S1: ^{1}H-NMR spectrum of **1** in DMSO-d_6 at room temperature.
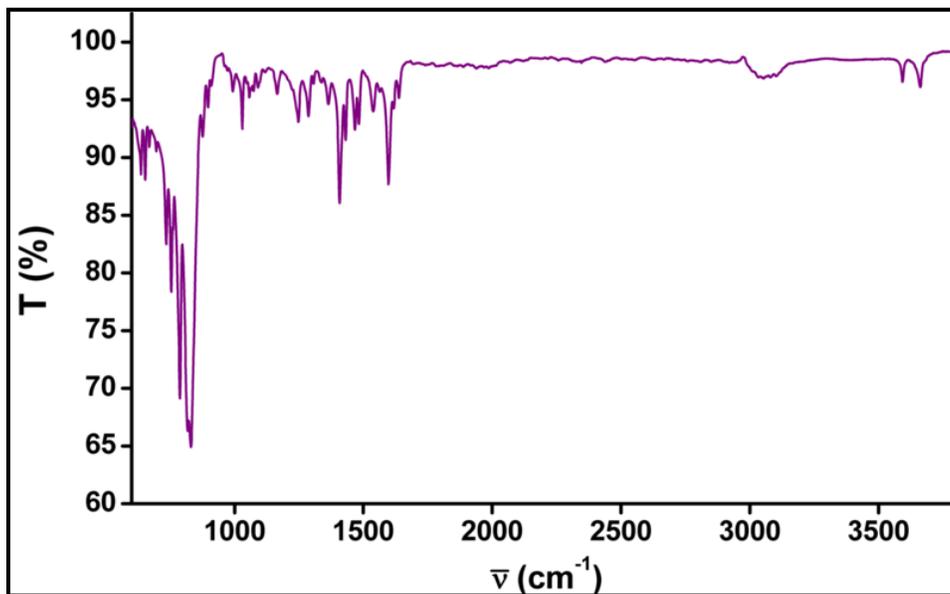
Figure S2: FTIR spectrum of **1** in KBr medium.
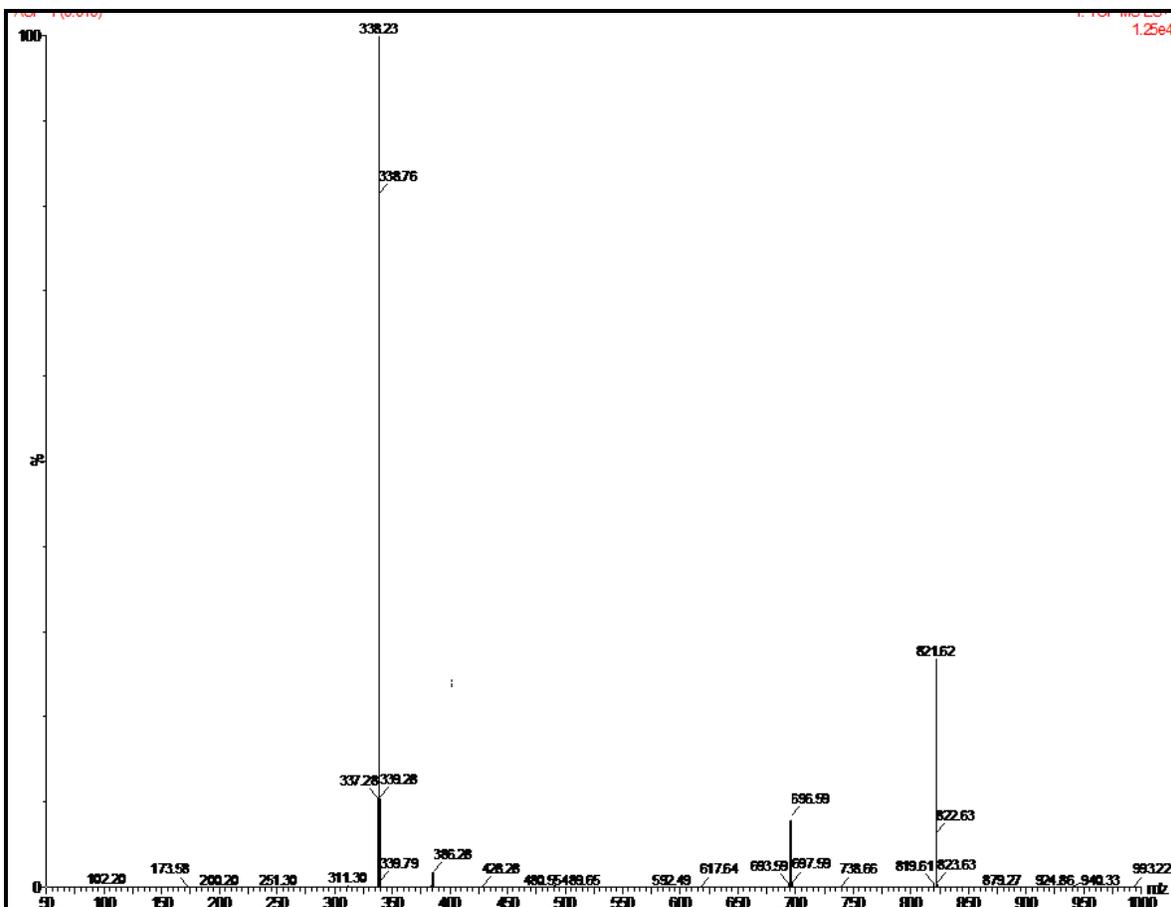
Figure S3: TOF-MS spectrum of **1**.
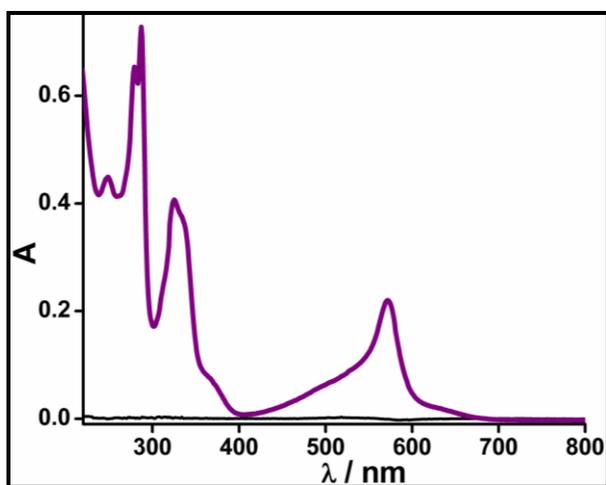
Figure S4: UV-vis spectrum of **1** (10^{-5} M, CH_3CN) at room temperature.
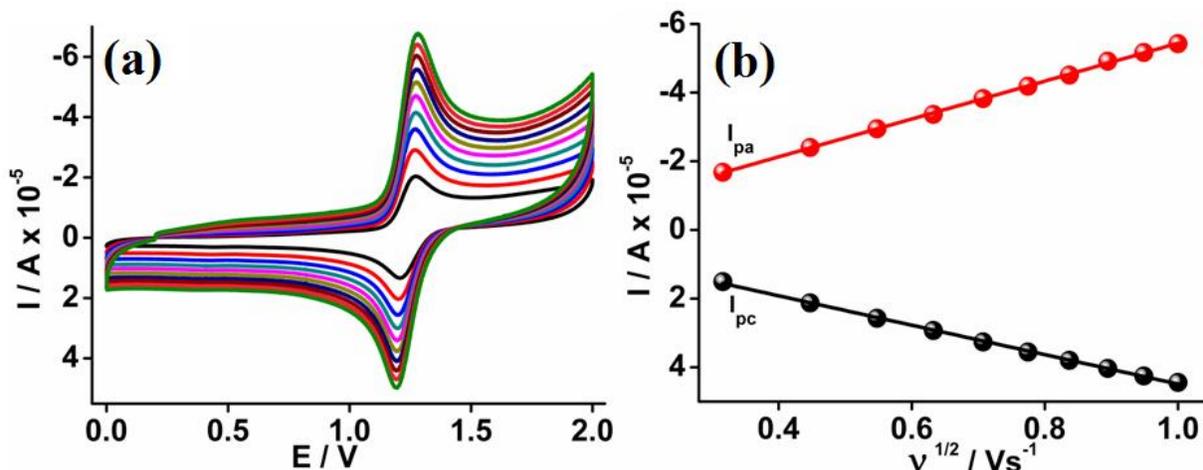
Figure S5: (a) Cyclic voltammogram of **1** (1×10^{-3} M) in CH_3CN containing 0.1 M Bu_4NPF_6 at scan rates ranging from 100 to 1000 mV. The glassy carbon was used as the working electrode, platinum wire as counter electrode and aqueous Ag/AgCl as reference electrode. (b) Plot of current density as a function of square root of scan rate ($R^2 = 0.99$).

Preparation of ppm-level solutions. A stock solution of 1000 ppm of various salts of KCN, KF, KNO_3, KNO_2, KSCN, K_2SO_4, NH_4PF_6, $NaClO_4$, $KHCO_3$, NaOAc, KI, KBr, KCl, K_2CO_3, $AgNO_3$, $FeCl_3$, $LiNO_3$, $NiCl_2.6H_2O$, $MnCl_2.4H_2O$, $CuCl_2.2H_2O$, $CoCl_2.6H_2O$, $Pb(NO_3)_2$, $FeSO_4.7H_2O$ and $Hg(NO_3)_2.H_2O$ were made by dissolving 10 mg of each salts in 10 ml of suitable solvents, water for aqueous medium and mixture of dry solvents *i.e.,* acetonitrile/ethanol/DMSO for non-aqueous medium. Furthermore, the stock solution was diluted to 1 ppm by taking 5µl volume of stock solution (1000 ppm) and making up it in solution of **1** upto 5 ml. The solution was used for analyses. For proof-of-concept experiments, pool and tap water samples were collected and filtered before preparing stock solution (1000 ppm) of CN^-/F^-.

Detection procedure of ppm-levels of CN^- and F^-: A 5 ml solution of **1** (10^{-5} M, CH_3CN) was treated with 5µl stock solution (1000 ppm) of CN^-/F^- (1.0 ppm in acetonitrile solution of **1**), mixed well within seconds. The resulting solution was used for recording absorbance and emission spectra at room temperature. The similar methodology was executed for higher concentrations of CN^- and F^-.
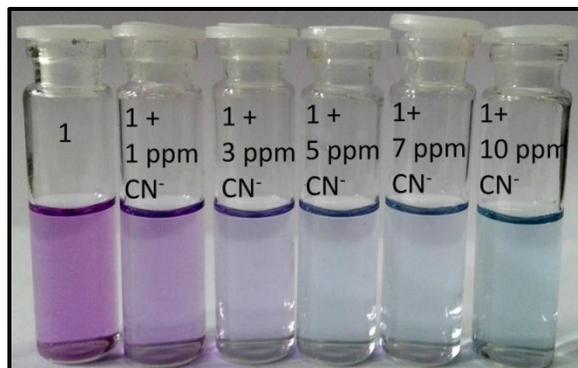
Figure S6: Visual colour changes in the solution of **1** (10^{-5} M, CH₃CN) on addition of 1-10 ppm of CN⁻ in H₂O.

Figure S7: Visual colour changes in the solution of **1** (10^{-5} M, CH₃CN) on addition of 2-15 ppm of F⁻ in H₂O.
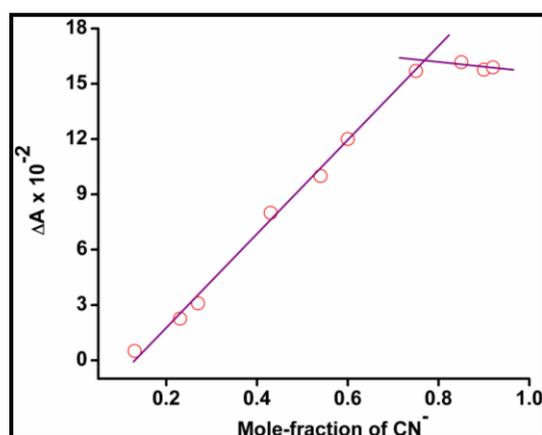
Figure S8: Job's plot for varying mole-fraction of CN⁻ in **1** (10^{-5} M, CH₃CN) at $\lambda = 569$ nm.
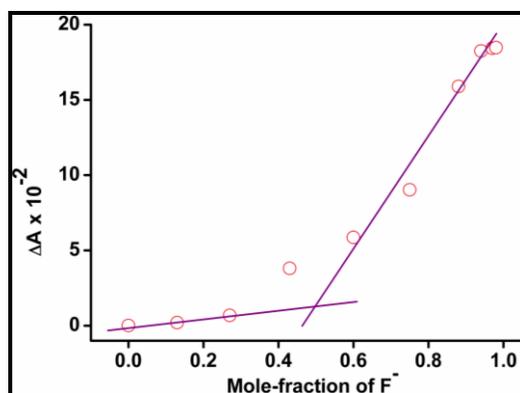
Figure S9: Job's plot for varying mole-fraction of F^- in **1** (10^{-5} M, CH_3CN) at $\lambda = 569$ nm.
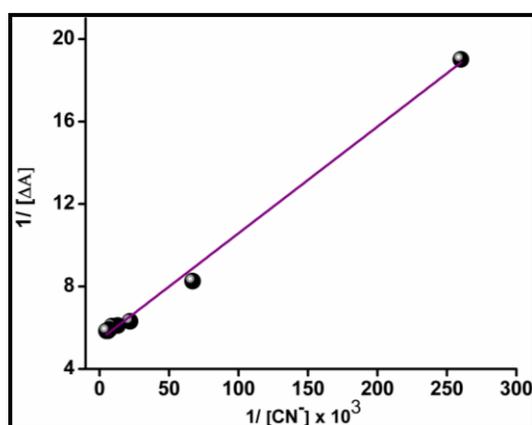
Figure S10: Benesi-Hildebrand plot showing reciprocal of change in absorption of **1** *vs.* reciprocal of concentration of CN^- ($R^2 = 0.99$) at $\lambda = 569$ nm.
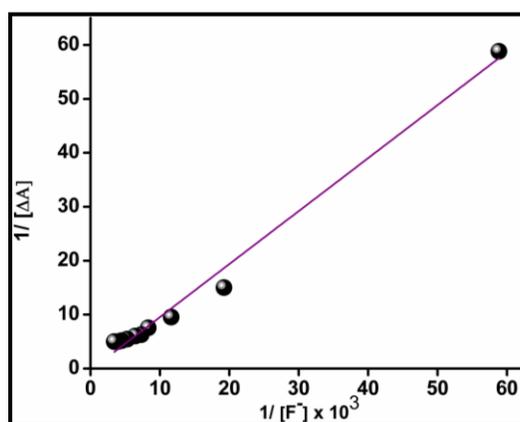
Figure S11: Benesi-Hildebrand plot showing reciprocal of change in absorption of **1** *vs.* reciprocal of concentration of F^- ($R^2 = 0.98$) at $\lambda = 569$ nm.
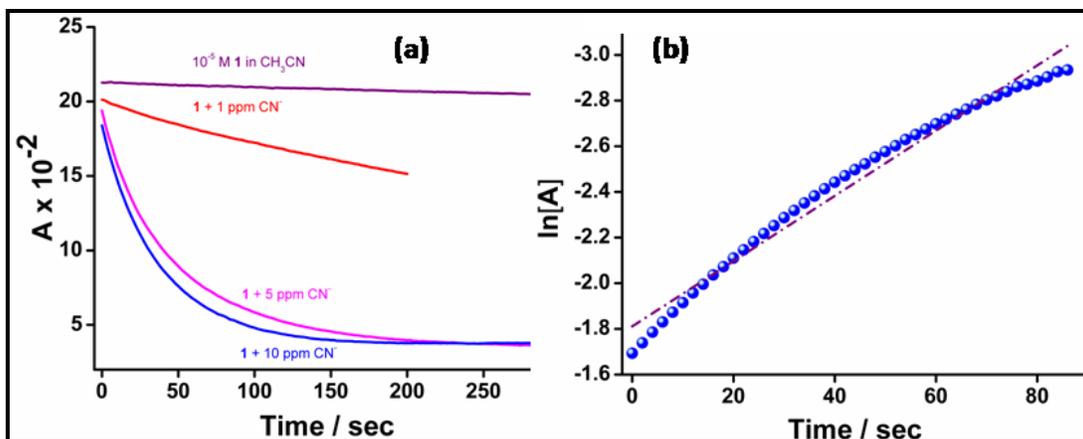
Figure S12: (a) Change in absorbance of **1** (10^{-5} M, CH$_3$CN) at λ = 569 nm upon addition of 1, 5 and 10 ppm of CN$^-$ in H$_2$O; (b) Representative plot between ln[A] *vs.* time (R^2 = 0.97).
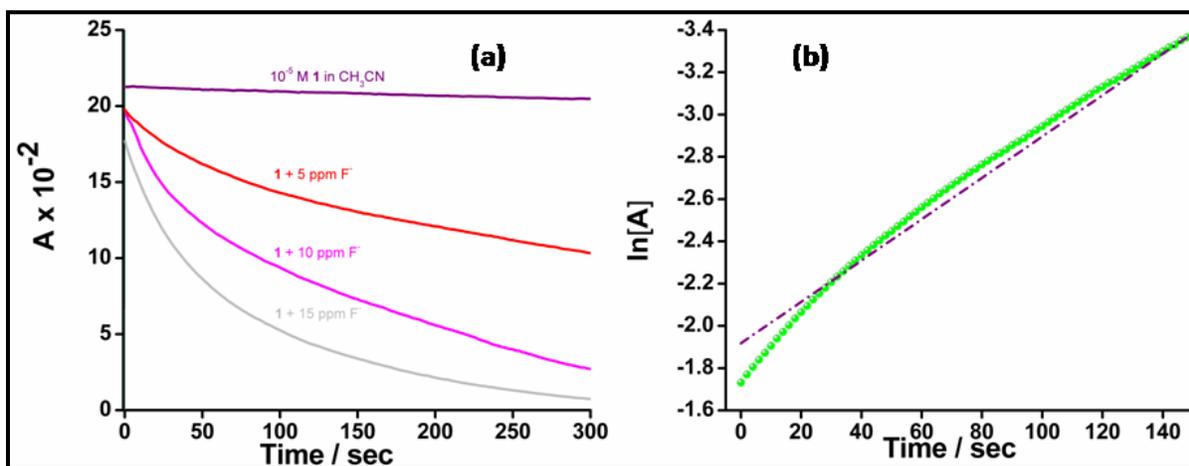
Figure S13: (a) Change in absorbance of **1** (10^{-5} M, CH$_3$CN) at λ = 569 nm upon addition of 5, 10 and 15 ppm of F$^-$ in H$_2$O; (b) Representative plot between ln[A] *vs.* time (R^2 = 0.99).

Figure S14: Visual colour changes in the solution of **1** (10^{-5} M, CH$_3$CN) on addition of 15 ppm of different anions in H$_2$O.
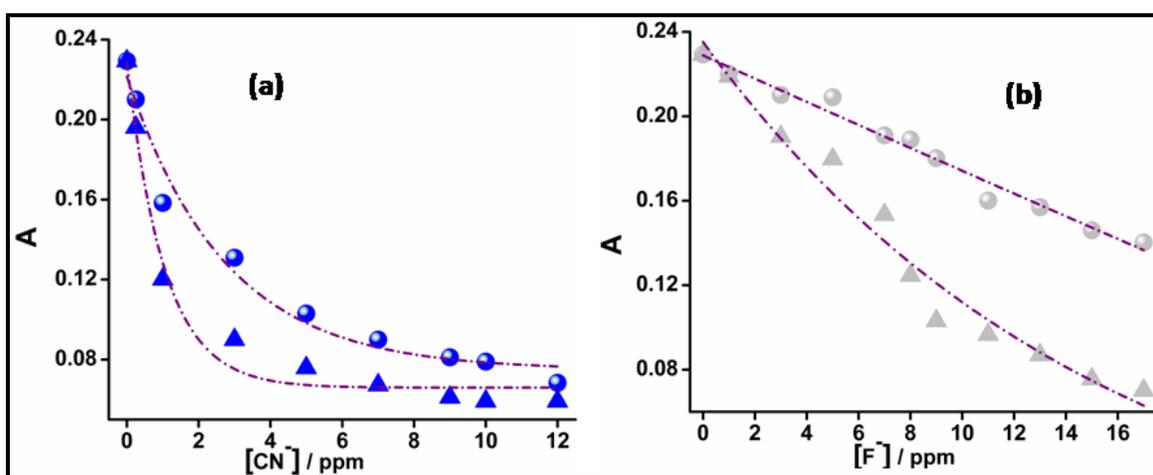
Figure S15: Proof-of-concept experiments with probe **1** (at $\lambda = 569$ nm) for determining (a) CN$^-$ in pool (blue balls, $R^2 = 0.97$) and tap water (blue triangles, $R^2 = 0.98$); (b) F$^-$ in pool (gray balls, $R^2 = 0.97$) and tap water (gray triangles, $R^2 = 0.96$) solutions.
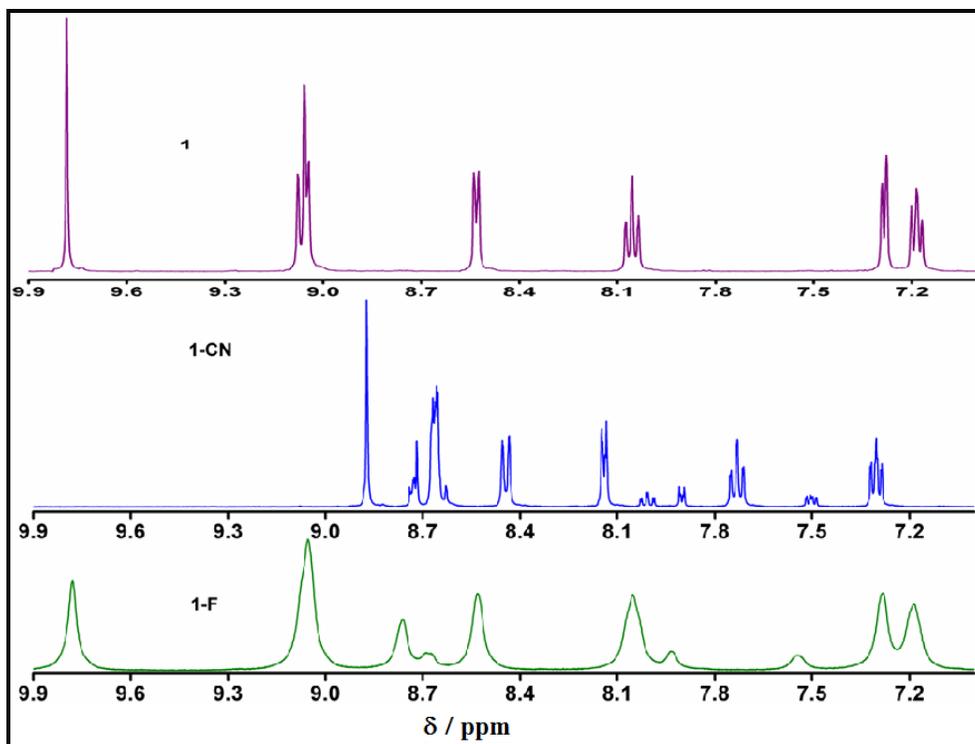
Figure S16: ^{1}H-NMR spectra of **1, 1-CN⁻** and **1-F⁻** in DMSO-d_6 at room temperature.
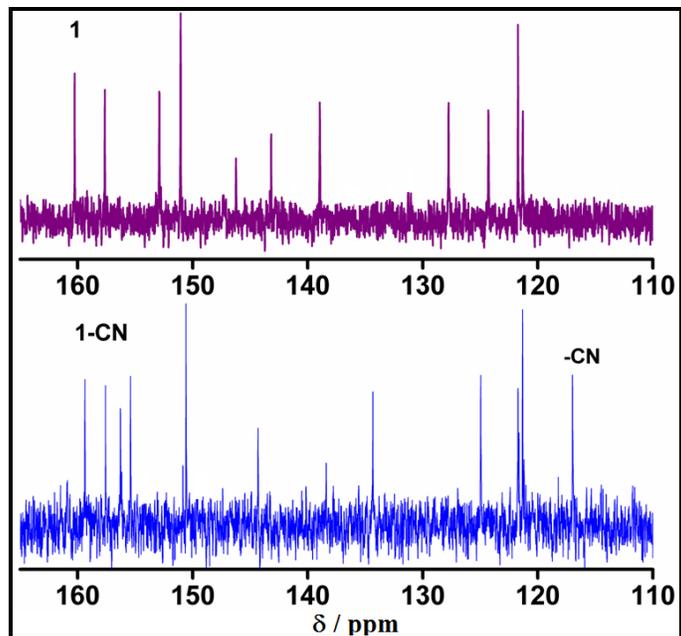
Figure S17: ^{13}C-NMR spectra of **1** and **1-CN⁻** in DMSO-d_6 at room temperature; ^{13}C-NMR of **1-CN⁻** (400 MHz, δ): 159.35, 157.26, 156.27, 155.39, 150.57, 144.31, 138.39, 134.34, 124.96, 121.64, 121.20, 116.97.
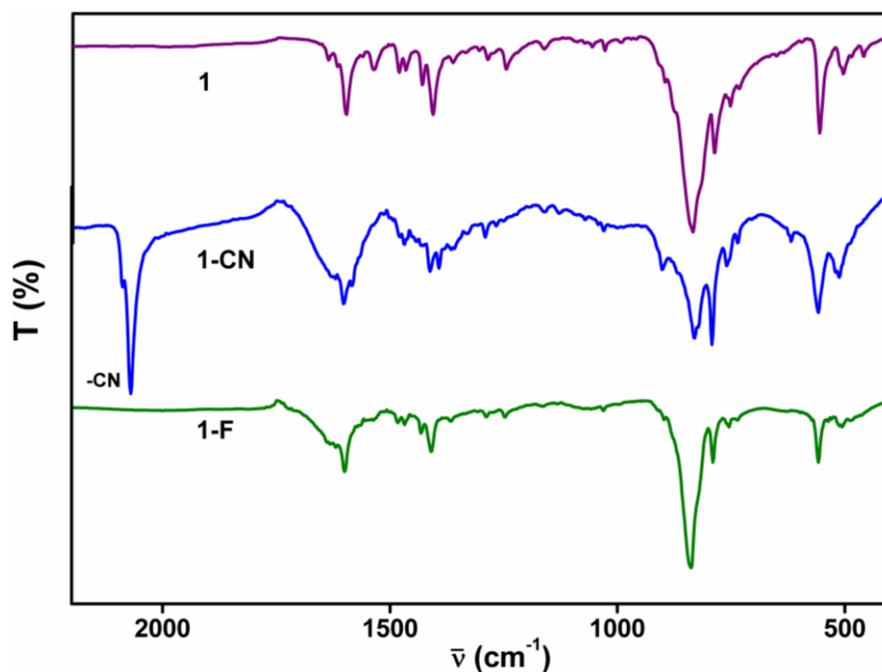
Figure S18: FTIR spectra of **1, 1-CN⁻** and **1-F⁻** in KBr medium.
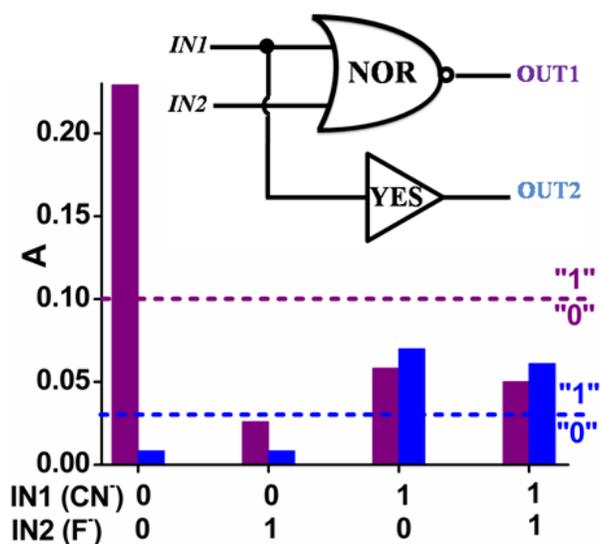
Figure S19: Absorbance outputs of **1** at $\lambda = 569$ nm in the presence of chemical inputs *viz.* IN1 (CN⁻) and IN2 (F⁻) and the corresponding two input combinatorial logic circuit. The purple and blue bars depict OUT1 ($\lambda = 569$ nm) and OUT2 ($\lambda = 413$ nm) respectively. Dotted lines represent the threshold level of absorbance outputs. Threshold level = 0.10 for OUT1 and 0.03 for OUT2. The output above the threshold level is read as "1" otherwise "0".
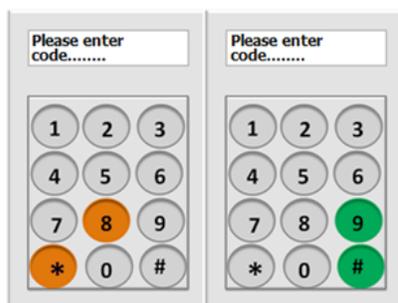
KEY	Absorbance at 569 nm	Output	KEY	Absorbance at 569 nm	Output
*0	OFF	0	#0	OFF	0
*1	OFF	0	#1	OFF	0
*2	OFF	0	#2	OFF	0
*3	OFF	0	#3	OFF	0
*4	OFF	0	#4	OFF	0
*5	OFF	0	#5	OFF	0
*6	OFF	0	#6	OFF	0
*7	OFF	0	#7	OFF	0
*8	ON	1	#8	OFF	0
*9	OFF	0	#9	ON	1

Figure S20: A molecular keypad lock with absorbance output at λ = 569 nm (Threshold level = 0.10). Only when the correct password "*8" (* = CN^-, 8 = Ag^+) or "#9" (# = F^-, 9 = Fe^{2+}) is entered absorbance channel is turned on. The table shows the outputs in the absorbance channel and the overall output in response to the different input combinations (* = CN^-, # = F^-, 0 = Cu^{2+}, 1 = Co^{2+}, 2 = Fe^{3+}, 3 = Li^+, 4 = Hg^{2+}, 5 = Pb^{2+}, 6 = Ni^{2+}, 7 = Mn^{2+}, 8= Ag^+, 9 = Fe^{2+}.

References:

S1. D. D. Perrin and W. L. F. Armarego, *Purification of Laboratory Chemicals*, 3. Aufl., Oxford. Pergamon Press, 1988.

S2. T. Duchanois, T. Etienne, M. Beley, X. Assfeld, E. A. Perpète, A. Monari and P. C. Gros, *Eur. J. Inorg. Chem.*, 2014, 3747.

S3. E. C. Constable and A. M. W. C. Thompson, *J. Chem. Soc. Dalton. Trans.,* 1992, 2947.